



**HAL**  
open science

# Pilot-scale direct UV-C photodegradation of pesticides in groundwater and recycled wastewater for agricultural use

S. Ferhi, Julien Vieillard, C. Garau, O. Poulter, L. Demey, R. Beaulieu, P. Penalva, V. Gobert, F. Portet-Koltalo

## ► To cite this version:

S. Ferhi, Julien Vieillard, C. Garau, O. Poulter, L. Demey, et al.. Pilot-scale direct UV-C photodegradation of pesticides in groundwater and recycled wastewater for agricultural use. *Journal of Environmental Chemical Engineering*, 2021, 9 (5), pp.106120. 10.1016/j.jece.2021.106120 . hal-04097462

**HAL Id: hal-04097462**

**<https://hal.science/hal-04097462v1>**

Submitted on 22 Aug 2023

**HAL** is a multi-disciplinary open access archive for the deposit and dissemination of scientific research documents, whether they are published or not. The documents may come from teaching and research institutions in France or abroad, or from public or private research centers.

L'archive ouverte pluridisciplinaire **HAL**, est destinée au dépôt et à la diffusion de documents scientifiques de niveau recherche, publiés ou non, émanant des établissements d'enseignement et de recherche français ou étrangers, des laboratoires publics ou privés.



Distributed under a Creative Commons Attribution - NonCommercial 4.0 International License

1 **Pilot-scale direct UV-C photodegradation of pesticides in groundwater and recycled**  
2 **wastewater for agricultural use.**

3 S. Ferhi<sup>1, 2</sup>, J. Vieillard<sup>2</sup>, C. Garau<sup>1, 2</sup>, O. Poulthier<sup>3</sup>, L. Demey<sup>4</sup>, R. Beaulieu<sup>1,5</sup>, P. Penalva<sup>6</sup>, V.  
4 Gobert<sup>4</sup>, F. Portet-Koltalo<sup>2, \*</sup>

5

6 1 Seed Innovation Protection Research Environment, Comité Nord – SIPRE, Rue des  
7 Champs Potez, 62217 Achicourt, France.

8 e-mails: [sabrina.ferhi@yahoo.fr](mailto:sabrina.ferhi@yahoo.fr); [charlene.garau@gmail.com](mailto:charlene.garau@gmail.com)

9 2 Normandie University, UNIROUEN, COBRA laboratory UMR CNRS 6014, 55 rue Saint  
10 Germain, 27000 Evreux, France.

11 e-mails: [florence.koltalo@univ-rouen.fr](mailto:florence.koltalo@univ-rouen.fr); [julien.vieillard@univ-rouen.fr](mailto:julien.vieillard@univ-rouen.fr)

12 3 CRT PRAXENS, 55 rue Saint Germain, 27000 Evreux, France

13 e-mail : [contact@praxens.fr](mailto:contact@praxens.fr); [n.picard@praxens.fr](mailto:n.picard@praxens.fr)

14 4 FN3PT/inov3PT, French Federation of Seed Potato Growers, Rue des Champs Potez,  
15 62217 Achicourt, France

16 e-mail: [laura.demey@inov3pt.fr](mailto:laura.demey@inov3pt.fr); [virginie.gobert@inov3pt.fr](mailto:virginie.gobert@inov3pt.fr)

17 5 Laboratoire de Glycochimie, des Antimicrobiens et des Agroressources (LG2A) CNRS  
18 UMR 7378, and Institut de Chimie de Picardie FR 3085, Université de Picardie - Jules Verne,  
19 80039 Amiens, France.

20 e-mail: [beaulieu.remi@yahoo.com](mailto:beaulieu.remi@yahoo.com)

21 6 Normandie Sécurité Sanitaire, 55 rue Saint Germain, 27000 Evreux, France.

22 e-mail: [contact@n2s.fr](mailto:contact@n2s.fr)

23

24 **\* Author to whom correspondence should be addressed:**

25 e-mail: [florence.koltalo@univ-rouen.fr](mailto:florence.koltalo@univ-rouen.fr) ; Tel.: +33-232-291-535; Fax: +33-232-291-539.

26

27 **Abstract**

28

29 Pesticides widely used for intensive agriculture may leach to groundwater and pose problems  
30 to drinking water and irrigation. UV-C disinfection systems (UV-DS) for water disinfection  
31 can be used also for the abatement of organic micropollutants. A pilot-scale continuous flow-  
32 through UV-DS system was evaluated for its degradation efficiency of atrazine (ATR),  
33 malathion (MAL) and glyphosate (GLY) from 40 L water. Groundwater used to irrigate  
34 potato fields and recycled wastewater used to wash potatoes were treated without catalysts to  
35 avoid any toxicity effect on potatoes. Chromatographic methods were used to quantify very  
36 low pesticide levels before and after UV-C treatments ( $<10 \mu\text{g L}^{-1}$ ), while a specific method  
37 was adapted to analyse traces of GLY ( $0.0008\text{-}10 \mu\text{g L}^{-1}$ ) in recycled wastewater containing  
38 suspended particulate matter (SPM). ATR was completely eliminated from groundwater after  
39 15 min photodegradation while 80% was removed from the turbid wastewater after 25 min.  
40 For MAL, 70-80% was removed in 25 minutes from the groundwater. For wastewater, the  
41 initial concentration was important for the performance of the photolytic process. An amount  
42 of 75% of GLY was eliminated after 10 minutes irradiation at concentrations higher than  
43 those found in natural groundwater. In wastewater, the UV-C treatment was less efficient  
44 because GLY was mainly adsorbed to SPM which obstruct the photodegradation process.  
45 Therefore, the pilot-scale UV-DS using a turbulent flow and a multiple-lamp system was  
46 performant to remove quantitatively traces of pesticides from large volumes of water, by  
47 direct photolytic oxidation, when the turbidity of the treated water was limited.

48

49 **Key words**

50 UV-C photolysis; recycled water; pesticides; glyphosate; pilot-scale treatment; ultra-trace  
51 analysis

52

53 **Abbreviations**

54

55 AOP: Advanced oxidation processes

56 AMPA: aminomethylphosphonic acid

57 ATR: Atrazine

58 CIP: Cleaning in place

59 DEA: Desethylatrazine

60 DI: Deionized

61 DIA: Deisopropyl-atrazine

62 DOM: Dissolved organic matter

63 FLD: Fluorescence detection

64 FMOC: Fluorenylmethoxycarbonyl

65 GC-MS: Gas chromatography coupled to mass spectrometry

66 GLY: Glyphosate

67 HA: Humic acids

68 IARC: International Agency for Research on Cancer

69 LC: Liquid chromatography

70 LOD: Limit of detection

71 LOQ: Limit of quantification

72 MAL: Malathion

73 SIP: Sterilization in place

74 S/N: Signal to noise

75 SPE: Solid phase extraction

76 SPM: Suspended particulate matter

77 UV-DS: UV disinfection systems

78

79 **1. Introduction**

80 The extension of intensive agriculture worldwide has led to an increase in the use of  
81 pesticides for plant and crop protection in the past decades and they have become among the  
82 most frequently occurring organic pollutants in surface and groundwater [1, 2]. A majority of  
83 pesticides are persistent and resist to natural degradation processes and so they remain for  
84 extended periods in soils (after field applications) where they can accumulate. Some  
85 pesticides may leach to groundwater and pose problems for drinking water and irrigation.  
86 Because of possible adverse effects on the environment and human health caused by a  
87 majority of pesticides, the European Union established a maximum permissible concentration  
88 of  $0.1 \mu\text{g L}^{-1}$  in drinking water for one target pesticide and a total concentration of  $0.5 \mu\text{g L}^{-1}$   
89 for the sum of them [3].

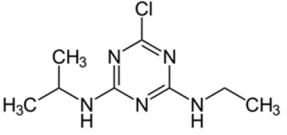
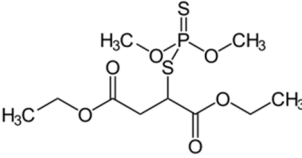
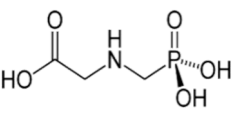
90 Each year in France, more than 5 billion  $\text{m}^3$  of water is collected for agricultural use, of which  
91 60% is used for irrigation. In potato production,  $0.6 \text{ m}^3$  water is required to produce 1 kg of  
92 potato tubers. In a context of sustainable development and to save drinking water, wastewater  
93 is expected to be recycled and reused, but the presence of pesticides above regulated  
94 concentrations can, as for irrigation water, pose a serious problem.

95 Atrazine (ATR) is one of the most commonly used herbicides in the world [4]. It is not  
96 volatile, not very polar and not very soluble in water, and it can accumulate onto soil organic  
97 matter (Table 1). Before its ban in France in 2003, the organochlorine ATR was commonly  
98 used in corn and wheat cultivation, but also in potato fields. ATR and two of its degradation  
99 products (desethylatrazine (DEA) and hydroxyatrazine) were among the most detected  
100 substances in the French rivers between 2009 and 2013 [5]. ATR is classified in group 3 of  
101 the International Agency for Research on Cancer (IARC), with an inadequate evidence for the  
102 carcinogenicity in humans but a sufficient evidence in experimental animals (Table 1).

103 After 2003, ATR was largely replaced by glyphosate (GLY) in France, which is now the most  
104 widely used herbicide and became (with its main transformation product  
105 aminomethylphosphonic acid (AMPA)) the most measured in French rivers [6]. GLY is a  
106 non-selective broad-spectrum organophosphate herbicide, not volatile, very polar and very  
107 soluble into water (Table 1). However, it can also accumulate into soils through the formation  
108 of complexes with soil cations, depending on soil pH [7]. In 2015, IARC classified GLY as  
109 “probably carcinogenic to humans” (Group 2A) (Table 1). GLY drifts can also cause leaf  
110 deformation of potato plants and can consequently lead to serious economic losses for  
111 impacted producers after lot rejections. Just like GLY, malathion (MAL) is an  
112 organophosphorous compound but is generally used as an insecticide. As ATR, MAL is  
113 neither volatile, nor being very polar and not very soluble into water, so it can accumulate  
114 onto soil organic matter (Table 1). It has been forbidden in France since 2007, but it was  
115 previously used to eliminate fungi from seed potato lots. Even if it is no more a major  
116 pesticide found in French rivers, it is a dangerous persistent compound, which has been  
117 classified as “probably carcinogenic to humans” (Group 2A) by IARC (Table 1), as one of its  
118 transformation product malaaxon.

119 Table 1: Physico-chemical and carcinogenic characteristics of the studied pesticides

120

	Atrazine	Malathion	Glyphosate
Chemical structure			
pKa	1.64	-	2.34; 5.73; 10.2
Vapour Pressure (25°C) (Pa)	$3.85 \times 10^{-5}$	$4.5 \times 10^{-4}$	$1.31 \times 10^{-5}$
Solubility (20°C) (mg L <sup>-1</sup> )	30	145	10,500 (pH=2)
Log K <sub>ow</sub>	2.5	2.8	-3.2 (pH=5-9)
K <sub>oc</sub> (L kg <sup>-1</sup> )	86	151-308	81-7564
Maximal absorption wavelength (nm)	225 [8]	210 [8]	< 200 (pH=7) [9]
Carcinogenicity (IARC)	Group 3	Group 2A	Group 2A

121

122

123 As pesticides can adversely impact aquatic environment at low levels and must be analysed at  
124 trace levels in groundwater as well as in drinking water, sensitive analytical methods must be  
125 developed. ATR and MAL can be analysed using liquid chromatography (LC) or gas  
126 chromatography coupled to mass spectrometry detection (GC-MS) but a pre-enrichment  
127 procedure (using solid phase extraction (SPE) for example) is generally required to reach  
128 concentrations lower than  $0.1 \mu\text{g L}^{-1}$  [10-12]. GLY and AMPA are generally analysed using  
129 LC coupled to MS or to fluorescence detection (FLD), but they can also be analysed using  
130 GC requiring previous derivatization [13-15]. As for ATR and MAL, various preparation  
131 steps must be developed before analysis (SPE, lyophilisation, large volume injections...) to  
132 analyse GLY and AMPA at trace levels [16-19].

133 Ultraviolet (UV) radiation-based processes are feasible treatment solutions to eliminate or  
134 drastically decrease a broad range of persistent organic pollutants such as pesticides in  
135 aqueous effluents. UV-C direct photolysis has been reported to achieve better degradation of  
136 persistent organic compounds than UV-A due to its higher energy [20, 21]. Photolysis  
137 processes include direct photolysis of compounds that are excited by absorbing energy from  
138 UV-C photons (180-280 nm) resulting in bond cleavage or rearrangement. ATR, MAL and  
139 GLY can potentially absorb such energies and could be possibly degraded (Table 1). But  
140 indirect photolysis can also occur when photons are absorbed by photoactive compounds  
141 producing reactive oxygen species (ROS) or dissolved organic matter (DOM) in excited state  
142 [22]. The application of a photocatalyst in advanced oxidation processes (AOPs) can enhance  
143 the degradation of too stable or photo-inactive compounds by a significant increase of the  
144 generation of ROS that oxidize and degrade them [23, 24]. UV-C disinfection systems (UV-  
145 DS) can be simultaneously used for water disinfection (eliminating pathogens) [25] but also  
146 for the abatement of organic micropollutants in water. The lower generation of toxic  
147 byproducts during the process compared to AOPs using catalysts can be an advantage of UV-



148 DS to treat aqueous effluents in contact with food or vegetables [26]. For example, the UV-C  
149 treatment of MAL in presence of TiO<sub>2</sub> catalyst produces more phosphate byproduct, which  
150 can be toxic [27].

151 In some agricultural practices, cooperatives ensure the reception of tons of potatoes that must  
152 be washed before their conditioning and delivery. Potatoes tubers are washed with natural  
153 groundwater and then wastewater is intended to be continuously collected and recycled for  
154 subsequent potatoes tubers cleaning, in order to save thousands cubic meters of water and to  
155 develop a circular economic model. In such current process, leached persistent pesticides can  
156 accumulate after few washing cycles, leading to significant exceedance of tolerated levels.  
157 UV-DS can be a promising technology to eliminate leached pesticides from wastewater in  
158 order to reuse it after each washing cycle. But continuous flow-through UV-DS reported  
159 experiments are rare and their degradation efficiency are not well known [28]. Moreover, the  
160 scaling up of photolysis or photocatalytic reactors is limited and studies are required for  
161 testing large-scale photodegradation processes and determining kinetic models for a variety of  
162 aqueous effluents, particularly natural water containing mixtures of persistent pollutants [29].

163 In this study, a pilot-scale disinfection process using UV-C irradiation for treating water in a  
164 continuous flow-through system was evaluated for the first time for its degradation efficiency  
165 of three pesticides, ATR, MAL and GLY (and some of their transformation products).  
166 Groundwater used to irrigate potato fields and recycled wastewater used to wash potatoes  
167 were treated. No chemical catalyst was introduced to avoid any interaction with potatoes used  
168 for animal or human feed. The disappearance kinetics of the three targeted compounds were  
169 established. In the case of GLY/AMPA a new SPE-HPLC-Fluorimetry analytical method had  
170 to be developed to reach ultra-trace levels in water containing solid particulate matter.

171

## 172 **2. Material and methods**

173 **2.1 Materials**

174 2.1.1 Chemicals

175 Standards of ATR, MAL, deisopropyl-atrazine (DIA), diethyl-atrazine (DEA), malaoxon,  
176 isomalathion and fluorenylmethoxycarbonyl chloride (FMOC-Cl) were obtained from Sigma  
177 Aldrich (Saint Quentin Fallavier, France). GLY, AMPA, derivatized GLY-FMOC and  
178 AMPA-FMOC were from Dr Ehrenstorfer GmbH (Augsburg, Germany). Deuterated labelled  
179 analytical standards atrazine-d5 (ATR-d5) and malathion-d10 (MAL-d10) were from Sigma  
180 Aldrich.

181 The LC grade solvents acetonitrile, dichloromethane, methanol and ethylacetate were  
182 purchased from Fischer Scientific (Illkirsh, France) while octanol was from Sigma Aldrich.  
183 Boric acid, sodium bicarbonate and formate ammonium were from Fisher Scientific.  
184 Potassium chloride and sodium hydroxide were from Sigma Aldrich, while disodium EDTA  
185 was from VWR (Strasbourg, France). Formate ammonium buffer 10 mM (pH 8) was prepared  
186 by mixing 10 mL of formate ammonium 1 M and 6.19 mL of sodium hydroxide 1 M in 1 L  
187 pure deionized (DI) water. Borate buffer 0.3 M (pH 8.7) was prepared by mixing 25 mL of a  
188 solution of boric acid and potassium chloride (0.3 M each) with 10.7 mL of sodium hydroxide  
189 0.3 M in 100 mL DI water.

190 Oxy-Anios 5 (Laboratoires ANIOS, France), the solution used to clean the UV-C pilot, was a  
191 solution of peracetic acid (48 mg g<sup>-1</sup>) and hydrogen peroxide (255.9 mg g<sup>-1</sup>).

192

193 2.1.2 Water sampling

194 Pure DI water was supplied by a Milli-Q water system (Fisher Scientific). A large volume of  
195 drilling water as well as wastewater from potato tubers cleaning was necessary to conduct the  
196 pilot study. Drilled water used for irrigation of potato crops was sampled from a potato field  
197 area near Evreux, Normandy France. Direct access to the drilling point was possible and

198 sampling was done with the aid of a lance. A description of the drilling point is presented in  
199 Figure S1 (supplementary materials). Groundwater is commonly used for crop irrigation due  
200 to its high degree of purity as a result of natural filtration through the soil. However, in recent  
201 years pure groundwater has become increasingly scarce due to drought and/or otherwise,  
202 contaminated by pesticide residues. Groundwater had a pH of 8.2, a mean conductivity of  
203  $0.453 \pm 0.006 \text{ mS cm}^{-1}$  (n=9) and a mean turbidity of  $21.6 \pm 3.0 \text{ FTU}$  (n=9). Compared with  
204 typical French tap water (turbidity  $\leq 2 \text{ FTU}$  and  $0.180 \leq \text{conductivity} \leq 1 \text{ mS cm}^{-1}$ , quality  
205 reference values from 2001-1220 French decree), the collected groundwater was slightly  
206 turbid and contained few ionized mineral salts.

207 Wastewater from potato tuber cleaning was sampled with a pump, which was inserted into a  
208 clean settled reservoir that collects wastewater from a potato packaging company. The  
209 reservoir is made up of four water pools which are inter-connected. As such, movement of the  
210 wastewater from the potatoes cleaning point crosses the four water pools, with debris settling  
211 in each of the pools, thus water arriving at the last pool is clearer and is intended be reused for  
212 cleaning potato tubers. Apart from this pre-treatment step, there was no additional treatment  
213 applied to the wastewater. As such, it is possible that all potato crop-related treatments and  
214 microbial contaminants or pathogens of the potato tubers maybe leached into the reservoirs,  
215 leading to an accumulation of pesticides and proliferation of pathogens. It is why the  
216 SurePure Turbulator<sup>TM</sup> device was expected to be installed after the last reservoir for an  
217 additional treatment of the washing water (Figure S2). Wastewater had a pH of 7.9, a mean  
218 conductivity of  $0.477 \pm 0.020 \text{ mS cm}^{-1}$  (n=9) and a mean turbidity of  $492 \pm 91 \text{ FTU}$  (n=9). As  
219 compared with typical French tap water, the recycled water was very turbid and contained few  
220 ionized mineral salts.

221 After sampling, ground- or wastewater was stored at room temperature in 10 L plastic  
222 containers, previously rinsed to eliminate plastic debris and avoid any possible contamination  
223 of the samples before analyses.

224 After water collection at the outlet of the disinfection setup, ground- or waste-water was  
225 centrifuged at 10,000 g for 5 min to eliminate a maximum of suspended particulate matter  
226 (SPM).

227

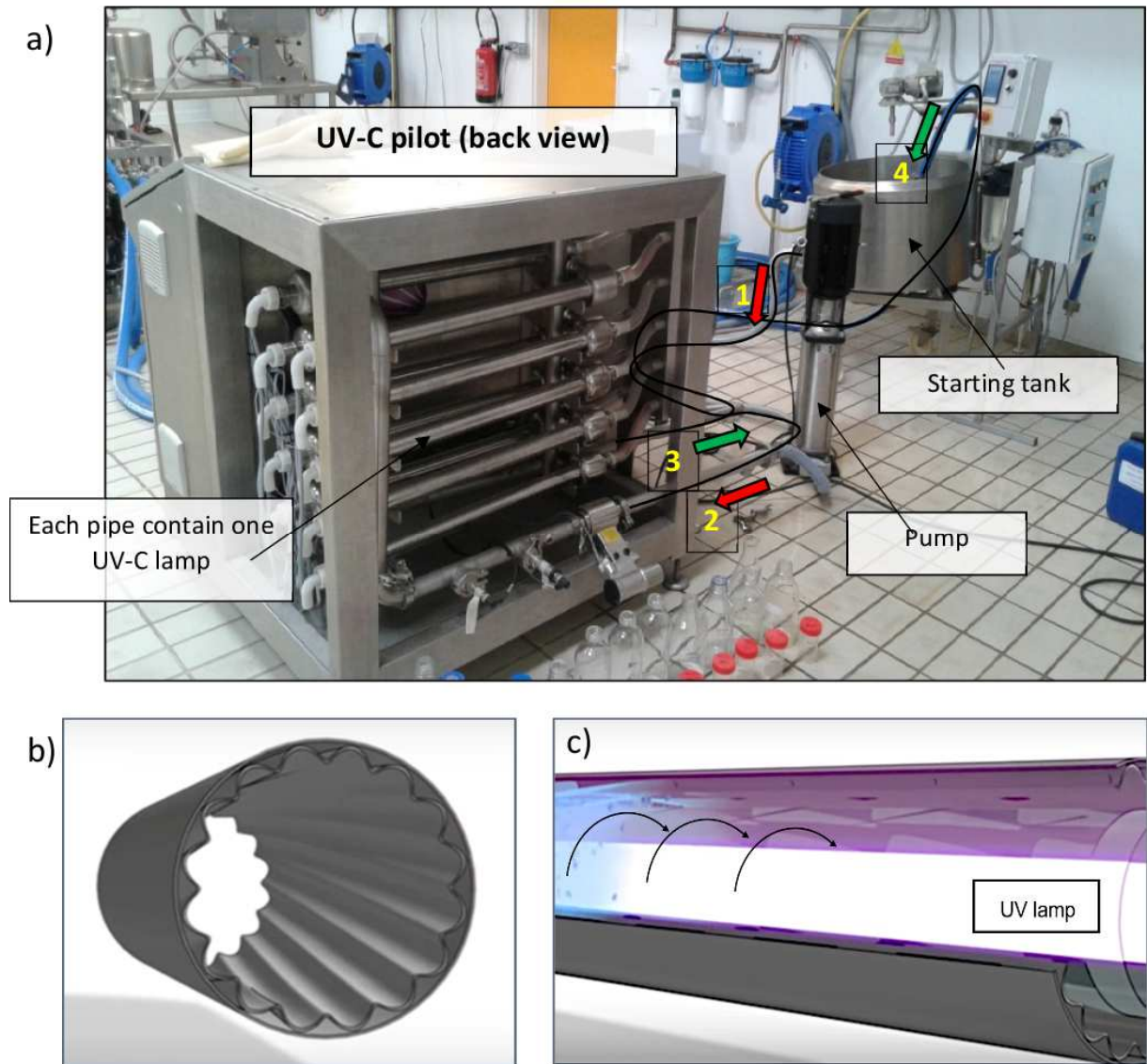
## 228 **2.2 Experimental disinfection setup and procedure**

### 229 2.2.1 Experimental setup

230 Fig. 1 shows the pilot-scale disinfection set-up (SurePure Europe). The patented SurePure  
231 Turbulator<sup>TM</sup> device exploits swirling turbulent flows and is designed for continuous flow of  
232 turbid fluids, so it is well adapted for treating complex solutions such as wine, blood, milk  
233 [30]. The turbulent flow and the multiple-lamp system (primarily used as germicide lamps)  
234 increase the liquid exposure to UV-C, limiting biofouling, enabling greater homogeneity and  
235 efficiency in purification. The disinfection pilot consists of a reservoir tank that can contain  
236 100 L water, of a liquid pump (flow-rate 4500 L h<sup>-1</sup>), of 10 quartz pipes of 80 cm long and 78  
237 mm diameter in a series circuit, each containing one mercury lamp (254 nm wavelength) (Fig.  
238 1). Each lamp is protected by a quartz sleeve and can deliver 36 W (which corresponds to 29  
239 W in the UV-C range), but with 15% loss due the quartz tubing material (measured and  
240 specified by the manufacturer).

241

242 Figure 1: (a) Pilot-scale disinfection UV-C pilot: “1” and “2” indicate the entrance water  
243 flow, “3” and “4” indicate the outlet flow; (b) 3D-modelling of the stainless steel tube; (c) the  
244 arrows indicate how the solution moves around the UV-C lamp.  
245



246

247

## 248 2.2.2 Photolytic experiments procedure

### 249 *Cleaning and sterilization in place (CIP and SIP steps):*

250 This procedure aimed at preparing the installation for the reception of the water to be treated.

251 It consisted of a chemical cleaning and decontamination using Oxy-Anios 5. In the starting  
252 tank, 200 mL of Oxy-Anios 5 (oxidizing agent) in 39.8 L water (0.5% mixture) was disposed.

253 This mixture flowed through the installation for 10 min with no light, passing through the  
254 pump and the pipes, then returning in the starting tank in a close circuit. After 10 min, the

255 installation was entirely rinsed with 100 L of tap water to eliminate any remaining Oxy-Anios  
256 5. Then the starting tank was again charged with 40 L of tap water which flowed for 10 min

257 through the machine but with lights switched on, in order to eliminate residual Oxy-Anios 5.

258 After rinsing, the water was eliminated and the machine was purged. At the end of each water  
259 treatment, the CIP and SIP steps were undertaken.

### 260 *Treatment step:*

261 To prevent some damages of the machine, especially of the quartz tubes, the water to be

262 treated was previously filtered through sieves of 450 and 250  $\mu\text{m}$ . The coarsest fractions of  
263 particulate matter were eliminated. The 40 L water samples (to be treated) were charged in the

264 starting tank, then the connection between the tank and the pump was opened and the water

265 circulation was switched on. During the first 5 min, the lamps were not switched on allowing  
266 the water to homogenize correctly in all the installation. As 32 seconds are required to flush

267 40 L of sample once in the tubes, 5 min was enough to reach a steady concentration after few  
268 circulation cycles [25]. As a control sample, a non-treated water sub-sample was collected

269 before the UV-C lamps were switched on. After each exposure time (1, 3, 5, 10, 15 and 25  
270 min), the lamps and the pump were stopped while 200 mL of sub-sample of treated water was

271 collected at the end-point of the pipes circuit. Then, the collecting point was closed and the  
272 lamp and the pump were restarted again until the next collection.

## 273 **2.3 Analytical methods**

### 274 2.3.1 Sample preparation and GC-MS analysis of ATR, MAL and some transformation 275 products

276 After water centrifugation, a preconcentration step was performed on the supernatant using  
277 solid phase extraction (SPE) with Oasis HLB 200 mg cartridges (Waters, Saint-Quentin-en-  
278 Yvelines, France). Solid phase conditioning was done with 6 mL dichloromethane, 6 mL  
279 acetonitrile followed by 6 mL DI water. The prepared water sample ( $V=200$  to  $1000$  mL) was  
280 passed through the SPE cartridge by a vacuum pump. The cartridge was finally dried by a  
281 nitrogen flow (1 h). The analytes were eluted with  $2\times 4$  mL dichloromethane. An amount of  
282  $10$   $\mu\text{L}$  octanol was added as solvent keeper and the eluate was evaporated to dryness  $45$  min  
283 at  $45^\circ\text{C}$  and  $200$  mBar (Mivac concentrator, Genevac, Fisher Scientific). At the end,  $170$   $\mu\text{L}$   
284 ethyl acetate was added alongside  $10$   $\mu\text{L}$  of internal standards of deuterated ATR-d5 and  
285 MAL-d10 (at  $100$   $\text{mg L}^{-1}$  in methanol). An aliquot of  $1$   $\mu\text{L}$  was injected (splitless mode,  
286  $280^\circ\text{C}$ ) into a gas chromatographer GC (7890B, Agilent, Santa Clara, USA), coupled with a  
287 mass spectrometer MS (7000C). Separation was performed using a  $60$   $\text{m}\times 0.25$  mm Zebron  
288 ZB- SemiVolatiles capillary column ( $0.25$   $\mu\text{m}$  film thickness) obtained from Phenomenex,  
289 with helium at  $1.4$   $\text{mL min}^{-1}$ . The oven temperature was programmed to begin at  $100^\circ\text{C}$  ( $1$   
290 min), increased to  $190^\circ\text{C}$  ( $30^\circ\text{C min}^{-1}$ ), then  $200^\circ\text{C}$  ( $0.8^\circ\text{C min}^{-1}$ ),  $230^\circ\text{C}$  ( $5^\circ\text{C min}^{-1}$ ) and  
291 finally  $240^\circ\text{C}$  ( $4^\circ\text{C min}^{-1}$ ). The MS detector operated at  $70$  eV. Quantification was based on  
292 selected ion monitoring for better sensitivity. The linearity of the detection was in the range  
293  $0.1$ - $8$   $\text{mg L}^{-1}$  for ATR, MAL, DEA, DIA, malaoxon, isomalathion, with  $r^2 > 0.995$  for  
294 calibration curves. Limits of detection (LOD) (signal to noise  $S/N=3$ ) and quantification  
295 (LOQ) ( $S/N=10$ ) of these compounds were evaluated on real samples of recycled wastewater  
296 ( $V=1000$  mL) spiked with  $2$   $\mu\text{g L}^{-1}$  of ATR, MAL and some transformation products (Table  
297 2). Their recoveries were in the range  $75$ - $106\%$  (Table 2).

298 Table 2: Limits of detection, of quantification and recovery yields for the different pesticides  
299 and some transformation products spiked in the turbid wastewater and analysed after SPE  
300 concentration.

301

	LOD (ng L <sup>-1</sup> )	LOQ (ng L <sup>-1</sup> )	Recoveries (%) (n=5)
ATR	0.71	2.6	78.0±9.6
DIA	1.3	4.1	106.0±8.7
DEA	0.3	1.9	75.0±9.3
MAL	0.1	2.3	95.0±16.5
Malaoxon	0.5	2.5	98.0±13.7
Isomalathion	2.8	8.6	90.0±18.7
GLY *	0.25	0.84	58.0 (n= 3)

302 \* Results obtained from spiked groundwater, only for GLY.

303



304 2.3.2. Sample preparation and LC-FLD analysis of GLY and AMPA

305 After water centrifugation and before the preconcentration step, 8 mL of EDTA 0.1 M  
306 (pH=10, adjusted with NaOH 5M) was added to 200 mL of the aqueous supernatant and was  
307 homogenized prior to filtration through a cellulose acetate filter (5-8  $\mu\text{m}$ , Fisher Scientific)  
308 under vacuum. The preconcentration step was performed using a PSOH Chromabond (500  
309 mg) SPE cartridges (Macherey Nagel, Hoerdt, France). Solid phase conditioning was done  
310 with 2 $\times$ 2 mL DI water, then 2 $\times$ 1 mL sodium bicarbonate (1 M) followed by 2 $\times$ 2 mL DI  
311 water. Then the water sample mixed with EDTA was passed through the SPE cartridge with  
312 the aid of a vacuum pump. After drying the cartridge under N<sub>2</sub> flow, analytes were eluted with  
313 2 $\times$ 1 mL KCl 1 M.

314 For the derivatization step, 0.4 mL borate buffer 0.3 M (pH 8.7) was added to the eluate and  
315 shaken for 20 s. Then 0.4 mL of FMOC-Cl (6 mM into acetonitrile) was added and the  
316 mixture was shaken in darkness for 20 min. Thereafter, 3 $\times$ 1 mL ethyl acetate were added and  
317 after shaking, the lower aqueous phase was recovered and analysed using LC (Beckman Gold  
318 126, Villepinte, France) coupled with a fluorimetric (FLD) detector Prostar 363 Varian  
319 (Agilent). An amount of 20  $\mu\text{L}$  of sample was injected into a Gemini C<sub>18</sub> column (150 $\times$ 4.6  
320 mm,  $d_p$ =5  $\mu\text{m}$ ) (Phenomenex), at 30°C and with a flow-rate of 1 mL min<sup>-1</sup>. The mobile phase  
321 was composed of solutions (A) (ammonium formate 10 mM, pH 9.5) and (B) (acetonitrile).  
322 The analysis began with 15% (B) for 5 min, followed by a linear gradient to 98% (B) over 15  
323 min before stabilizing at 98% (B) over 5 min. Optimal fluorescence excitation/emission  
324 wavelengths were, respectively, 250/310 nm to obtain a sensitive detection. The linearity of  
325 the detection was in the range 1-30  $\mu\text{g L}^{-1}$  for GLY and AMPA, with  $r^2$ >0.997 for calibration  
326 curves. The LOD, LOQ and recoveries are discussed in the section 3.1 (Table 2).

327

### 328 **3. Results and discussion**

#### 329 **3.1. Adaptation of the analytical methodology for the analysis of GLY at ultra-trace** 330 **levels in wastewater.**

331 GLY is often analysed at trace levels in drinking, surface water or groundwater, which do not  
332 contain high amounts of SPM or DOM and rarely in raw turbid water, where it has been  
333 demonstrated that GLY can be associated to particulate matter [17, 18, 31]. However, in the  
334 present study, although filtration and centrifugation were performed before analysis of the  
335 turbid recycled wastewater, organic colloids (DOM) and nano- or micro-particles from SPM  
336 could not be fully removed. Thus, there was a requirement for the development of new  
337 strategies in the sample preparation to analyse GLY at ultra-trace levels in turbid water. It was  
338 particularly critical to quantify GLY at concentrations in the  $\mu\text{g L}^{-1}$  range as direct  
339 photodegradation processes in these low concentration ranges, encountered in environmental  
340 water effluents, are not well known.

341 As GLY and AMPA were detected through a fluorimetric detector, allowing higher sensitivity  
342 than UV or MS detectors, they were derivatized using an excess of FMOC-Cl, because it can  
343 also react with other amines or amino acids which may be present in recycled water. FMOC-  
344 Cl was prepared into acetonitrile to obtain better derivatization yields [32]. It is known that  
345 the reaction must be done in alkaline conditions and that derivatization yields increase when  
346 pH increase from 7.0 to 9.1, but here, a pH=8.7 was selected to avoid high hydrolysis of  
347 FMOC-Cl into FMOC-OH at more alkaline pH [33]. As GLY and AMPA were obtained after  
348 concentration of 200 mL water in 2 mL aqueous solutions containing concentrated KCl,  
349 several volumes (300-600  $\mu\text{L}$ ) and concentrations (0.125-0.3 M) of FMOC-Cl were tested.  
350 Even if higher amounts of FMOC-Cl favor the derivatization process, a medium volume (400  
351  $\mu\text{L}$ ) of the highest concentrated solution was selected to avoid sample dilution. At last, the  
352 best reaction time was determined allowing the formation of derivatized analytes without the

353 formation of secondary by-products. The reaction time was tested between 0-24 h [34, 35].  
354 No significant difference on derivatization yields was observed after 20 min reaction ( $p > 0.05$ ,  
355 Student test,  $n=3$ ) and after 1h, higher amounts of secondary by-products could be observed.  
356 Therefore, 20 min derivatization was selected, obtaining mean derivatized glyphosate (GLY-  
357 FMOC) yields of  $100.8 \pm 9.7\%$  ( $n=3$ ). Using DI water spiked with GLY and AMPA, the limit  
358 of detection (LOD) ( $S/N=3$ ) and of quantification (LOQ) ( $S/N=10$ ) using LC-FLD after  
359 derivatization were  $0.013 \mu\text{g L}^{-1}$  and  $0.040 \mu\text{g L}^{-1}$ , respectively, for GLY-FMOC and  $0.09 \mu\text{g}$   
360  $\text{L}^{-1}$  and  $0.30 \mu\text{g L}^{-1}$ , respectively, for AMPA-FMOC. A review on analytical methods used for  
361 GLY/AMPA analyses in water using LC-FLD mentioned current LODs between 0.01-0.1  $\mu\text{g}$   
362  $\text{L}^{-1}$  for both chemicals [36]. GLY had to be quantified into water at levels as low as  $0.1 \mu\text{g L}^{-1}$ ,  
363 so the attained LOQ could be considered satisfactory.

364 GLY spiked in turbid water can be lost, due to various sorption phenomena on solid materials.  
365 Therefore, a concentration process through SPE, allowing a concentration factor of 100, was  
366 developed to accurately determine ultra-traces of GLY. Derivatized GLY-FMOC and AMPA-  
367 FMOC are anionic species in a large alkaline pH range, so various anion exchange SPE  
368 cartridges were tested, such as Chromabond PSOH (strong anion exchanger in the  $\text{OH}^-$  form),  
369 Chromabond  $\text{NH}_2$  (weak anion exchanger with aminopropyl bonded material) and Oasis  
370 MAX (containing a mixed-mode polymeric sorbent with quaternary ammonium groups).  
371 Various eluting solvents were tested to desorb GLY from the SPE cartridges. With Oasis  
372 MAX, aqueous solutions containing HCl (0.5 M) or sodium citrate (0.6 M) were tested, and  
373 low or inconsistent recoveries ( $2 \pm 2\%$  and  $140 \pm 24\%$  ( $n=3$  replicates), respectively) for GLY-  
374 FMOC were obtained. The HCl acid was not a good eluting solvent for the further  
375 derivatization step whereas sodium citrate yielded a more favorable alkaline  $\text{pH}=8$ . With  
376 Chromabond  $\text{NH}_2$ , aqueous solutions containing sodium citrate (0.6 M) and a phosphate  
377 buffer (0.1 M,  $\text{pH}=8$ ) gave  $43 \pm 9\%$  and  $108 \pm 5\%$  recoveries, respectively ( $n=3$ ). Unfortunately,

378 the chromatographic resolution of AMPA-FMOC was deteriorated when phosphate buffer  
379 was used. With Chromabond PSOH, an aqueous phase containing KCl (1 M) was used as  
380 eluting solvent and gave a mean recovery of  $102\pm 6\%$  ( $n=3$ ). This latter combination for the  
381 SPE step was chosen rather than the combination involving Oasis MAX/sodium citrate  
382 because the relative standard deviation was lower. The reproducibility of the recovery yields  
383 for quantifying GLY at very low levels in spiked DI water after SPE, evaluated on 3 tests on  
384 different days, were  $91.9\pm 20.4\%$  and  $98.7\pm 8.7\%$  for GLY spiked at  $0.1\ \mu\text{g L}^{-1}$  and  $0.6\ \mu\text{g L}^{-1}$ ,  
385 respectively.

386 As previously mentioned, quantifying GLY in drilling or recycled wastewater appeared not so  
387 easy, as they contain more or less SPM/DOM which required an elimination before LC  
388 analysis. Several membrane filters were tested, with cellulose acetate, nylon or nitrocellulose  
389 materials which demonstrated 11%, 24% and 45% GLY loss, respectively. As such as, the  
390 filter had to be carefully chosen to accurately quantify GLY in raw water containing particles,  
391 and cellulose acetate material seemed appropriate. Moreover, even if ground- and wastewater  
392 were centrifuged after their collection at the outlet of the disinfection setup in order to  
393 eliminate SPM, mineral or organic colloids, they could not be totally eliminated. Mineral  
394 colloids could contain iron or aluminium oxides that can sorb GLY [37]. Also, it has been  
395 demonstrated that metal cations could interfere on the GLY and AMPA derivatization [17,  
396 38]. Therefore, EDTA was introduced after centrifugation to precipitate mineral colloids and  
397 associated bivalent metallic species in order to eliminate them with further filtration. In the  
398 best analytical conditions, GLY spiked at  $10\ \mu\text{g L}^{-1}$  into groundwater and placed into the  
399 disinfection pilot without irradiation, was quantified with 58% recovery (Table 2). The 42%  
400 loss could be attributed to the sorption of GLY onto SPM/colloids (which were eliminated  
401 through centrifugation, precipitation and filtration before analysis), but also to the sorption  
402 onto the surface of the inox and quartz material of the pilot.

403 Concerning wastewater which was highly turbid and contained much more SPM, initial  
404 concentrations of GLY were not negligible. From one collected in October 2017 and another  
405 collected in March 2018, mean concentrations of  $4.1 \pm 3.2 \mu\text{g L}^{-1}$  (n=5) and  $2.6 \pm 0.9 \mu\text{g L}^{-1}$   
406 (n=6), respectively, were measured. The main transformation product AMPA could not be  
407 detected in wastewater. In comparison, GLY was initially found in groundwater at  $0.3 \pm 0.2 \mu\text{g}$   
408  $\text{L}^{-1}$  (n=3) which is significantly lower ( $p < 0.05$ , Student test). Then GLY was spiked at  $10 \mu\text{g}$   
409  $\text{L}^{-1}$  into wastewater and placed into the disinfection pilot without irradiation: it was quantified  
410 with only 19% recovery. Compared with the results from groundwater, it is clear that an  
411 important quantity was sorbed onto the pilot surfaces and coatings, but also on the high  
412 amount of SPM/colloids and so could not be quantified in the dissolved aqueous fraction.  
413 Considering the moderate GLY losses related to the presence of SPM/DOM into  
414 groundwater, procedural LODs and LOQ using SPE and LC-FLD could be measured only  
415 from spiked groundwater and were  $0.84 \text{ ng L}^{-1}$  and  $0.25 \text{ ng L}^{-1}$ , respectively (Table 2). Thus,  
416 the very low LOQ values obtained for ATR, MAL and GLY (Table 2) allowed for the  
417 quantification of those pesticides at ultra-trace levels into water of various turbidity, even  
418 after their degradation following UV-C treatment.

419

## 420 **3.2. Degradation of pesticides using the pilot-scale disinfection process**

### 421 3.2.1. Energy of UV-C exposure per liter of treated water

422 The transmitted UV-C energy (or its power  $P_{\text{transmitted}}$  in  $\text{J s}^{-1}$ ) to the aqueous fluid through the  
423 quartz tubing could be calculated using equation (1), knowing the power of each UV lamp  
424 ( $P_{\text{UV lamp}}$ ):

$$425 P_{\text{transmitted}} = (P_{\text{UV lamp}} \times \%_{\text{Loss}}) \times \text{number of lamps} = (29 \times 0.85) \times 10 = 246.5 \text{ J s}^{-1} \quad (1)$$

426 The time ( $t_{\text{pass}}$  in s) needed for the passage of the volume of water to be treated in the machine  
427 could be calculated using equation (2):

428  $t_{\text{pass}} = \frac{(V_T \times 3600)}{4500} = \frac{(40 \times 3600)}{4500} = 32 \text{ s}$  (2)

429 Where  $V_T$  was the volume of water to treat (40 L) and  $V=4500$  L was the total volume of  
 430 water which could be delivered by the pump in 1 h.

431 The energy applied to the volume of water to treat ( $E_{\text{pass}}$  in  $\text{J L}^{-1}$ ) in one passage could be  
 432 calculated using equation (3):

433  $E_{\text{pass}} = \frac{(t_{\text{pass}} \times P_{\text{transmitted}})}{V_T} = \frac{(32 \times 246.5)}{40} = 197.2 \text{ J L}^{-1}$  (3)

434 We could then calculate the total energy of UV-C exposure ( $E_{\text{exposure}}$  in  $\text{J L}^{-1}$  or  $\text{kJ m}^{-3}$ )  
 435 (corresponding to the fluence) for each treatment time using equation (4):

436  $E_{\text{exposure}} = \frac{\text{time} \times E_{\text{pass}}}{t_{\text{pass}}}$  (4)

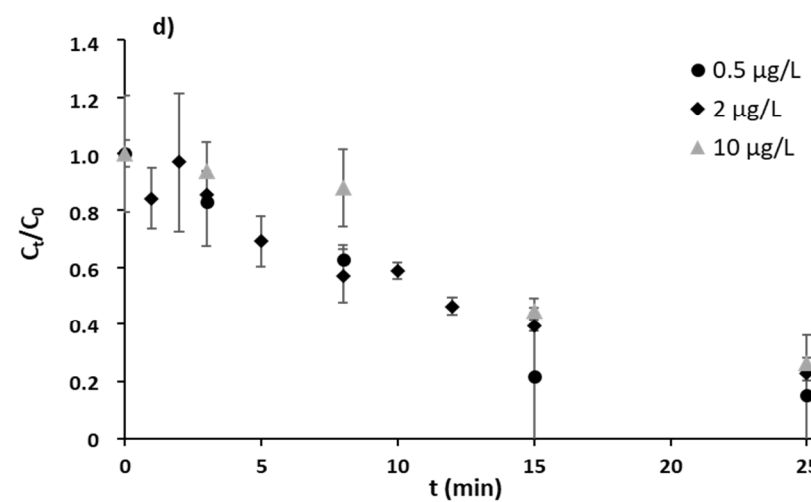
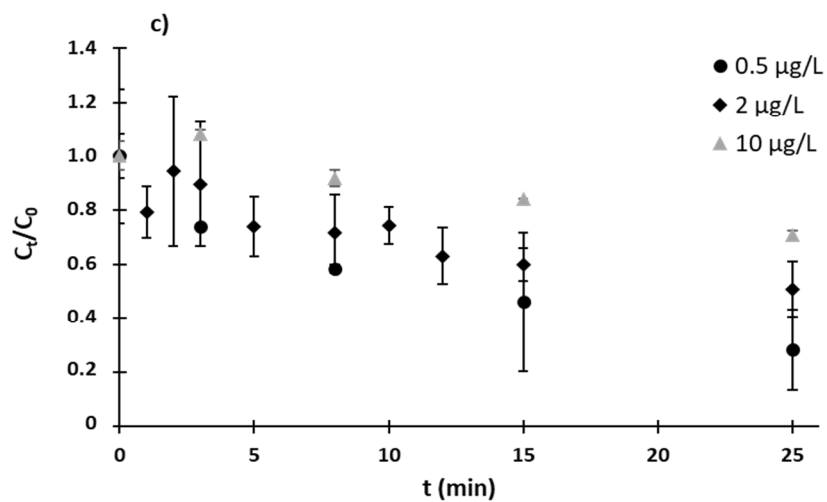
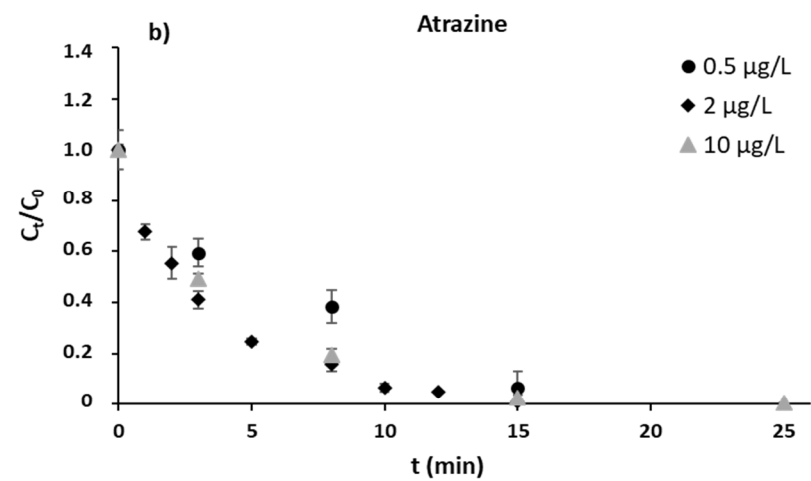
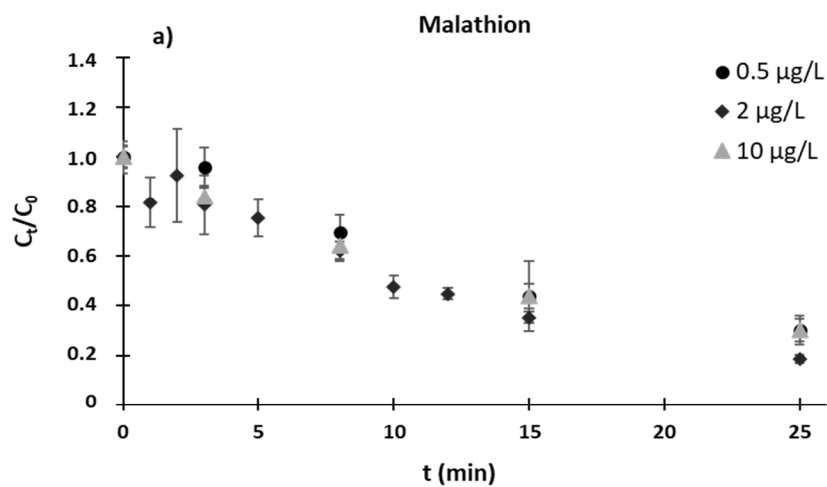
437 Where time is the treatment time (in min). Thus, the fluence could be calculated using a  
 438 simple equation (5):  $E_{\text{exposure}} = 369.75 \times \text{time}$  (5)

439

### 440 3.2.2 Dissipation of pesticides

#### 441 *Dissipation of atrazine and malathion*

442 The kinetic curves of ATR and MAL degradation were compared according to the water  
 443 treated. The measured relative concentrations ( $C_t/C_0$ ) are shown as a function of the  
 444 irradiation time on Fig. 2. The mean values of  $C_t/C_0$  were obtained through duplicate  
 445 experiments for a particular concentration of spiked pesticide, carried out on two different  
 446 days and using two different 40 L water sample cans, which explains the variability of the  
 447 results. As illustrated on equation (5), the longer the residence time into the UV-DS tubes, the  
 448 higher the energy delivered from the UV-C lamps. Both MAL and ATR were quantitatively  
 449 photodegraded by UV-C irradiation but a limit appeared after a few dozen minutes.



450

451 Figure 2: Plots of  $C_t/C_0$  versus photoreaction time for MAL and ATR in groundwater (a, b) and wastewater (c, d).  $C_0$  is the initial concentration

452 measured without irradiation ( $t=0$ ) and  $C_t$  is the measured concentration after  $t$  (min) irradiation ( $n=2$  experiments).

453 MAL and ATR could be dissipated through direct photolysis, but also through oxidation  
454 reaction with ROS. Indeed, in the case of UV-C irradiation, the water molecules can  
455 decompose in photoactive hydroxyl radicals that absorb the energy of irradiation [39]. The  
456 yield of this reactive intermediate can reach 0.280  $\mu\text{mol}$  per J of absorbed radiation energy  
457 [40]. In view of eq. (5), it was possible that 1760  $\mu\text{g L}^{-1}$  could be generated per min  
458 irradiation in the pilot, which is significantly above the concentrations of the dissolved  
459 pesticides to remove. Moreover, other oxidants such as superoxide radical or singlet oxygen  
460 could be generated: the big section of the turbulator device could help to oxygenize the  
461 aqueous solution during the process and promote these ROS formation [38].

462 More than 80% ATR could be eliminated in less than 25 minutes irradiation (corresponding to  
463 a fluence of 9244  $\text{kJ m}^{-3}$ , eq. (5)) irrespective of the quality of water treated and for all the  
464 tested concentrations, from 0.5 to 10  $\mu\text{g L}^{-1}$  (Fig. 2b and 2d). Only 15 minutes were necessary  
465 to completely eliminate ATR from the less turbid groundwater (fluence = 5546  $\text{kJ m}^{-3}$ ) (Fig.  
466 2.b). For wastewater the dissipation was limited to 80%. The larger amount of interfering  
467 compounds probably interacted with the ROS, limiting the efficiency of the oxidation reaction  
468 in the liquid phase. Also, the persistence of residual ATR which could not be eliminated after  
469 25 min irradiation was possibly due to their sorption onto SPM, where they were not  
470 accessible to direct irradiation.

471 It has been reported that DEA, DIA and 2-hydroxyatrazine are the main transformation  
472 products obtained by photolysis of ATR [41, 42]. These transformation products are obtained  
473 by excitation of the triazine, the dechlorination and the insertion of the hydroxyl radical  
474 generated by the water photolysis. As discussed, the GC-MS method was adapted to analyse  
475 ultra-traces of ATR and some of its current transformation products. The analysis of  
476 groundwater and wastewater before UV-C treatment demonstrated that ATR was not  
477 detectable ( $<0.00071 \mu\text{g L}^{-1}$ ), contrary to some of its transformation products. DEA was



478 detected ( $<0.002 \mu\text{g L}^{-1}$ ), and DIA could be quantified at  $0.15\pm 0.04 \mu\text{g L}^{-1}$  ( $n=4$ ) and  
479  $0.90\pm 0.20 \mu\text{g L}^{-1}$  ( $n=12$ ) in ground- and wastewater, respectively. Such contamination of  
480 natural water by ATR metabolites, produced from the metabolic activity of bacteria, has  
481 already been reported by Moreira *et al* [42]. After all the UV-C treatments, even the longer  
482 ones, DEA and DIA levels were not significantly changed in treated water compared with  
483 their initial concentrations. It is possible that the hydroxylation of the chlorinated carbon of  
484 ATR increased the stability of the chemical structure of these compounds [42]. Thus, DEA  
485 and DIA are difficult to remove by photolysis and it contributes to their prevalence and so to  
486 their wide detection in various water environments, even groundwater, and for decades after  
487 the phasing out of the parent molecule [43]. Also, Khan *et al.* [44] demonstrated that the  
488 degradation rate of DEA and DIA increased with the increase in their initial concentration  
489 when they were submitted to UV-C irradiation (254 nm). Therefore, their very low initial  
490 concentrations in ground- or wastewater might also explain why no DEA or DIA  
491 concentration change could be measured during the exposure to UV-C irradiation.

492 For MAL, the UV-C degradation was limited to 50-80% depending on water quality, for  
493 concentrations ranging from  $0.5$  to  $10 \mu\text{g L}^{-1}$  and after 25 min treatment (corresponding to a  
494 fluence of  $9244 \text{ kJ m}^{-3}$ ) (Fig. 2a and 2c). It has been reported that three oxidation by-products  
495 could be generated during photolysis [45]. The degradation of MAL could be initiated by the  
496 cleavage of the P-S bond to obtain the diethyl-2-mercaptosuccinate, and then the mercapto  
497 group was substituted by an hydroxyl group with the help of hydroxyl radicals, to obtain the  
498 diethyl malate and finally, the internal hydroxyl group could react with an hydrogen to give  
499 diethyl maleate [27]. The GC-MS analysis confirmed that malaoxon and isomalathion were  
500 not present, even at ultra-trace levels in water, before and after UV-C treatment, possibly  
501 because the P-S bond was rapidly cleaved by photolysis.

502 The results presented in Fig. 2 indicates that the degradation was more efficient in  
503 groundwater than in wastewater for both ATR and MAL. We could emphasize that SPM  
504 present in the unclear wastewater limits the interaction with photons involved in the  
505 photolysis and sorption protects pesticides from photolysis by competitive light attenuation  
506 [46]. Moreover, the largest amount of interfering compounds (DOM and inorganic ions) in  
507 wastewater should compete with ATR and MAL for photochemical reactions with ROS.  
508 Particularly, humic substances can reduce the pesticide photodegradation by a strong  
509 quenching effect and it can also quickly react with ROS [46, 47].

510 In both the tested water, ATR was more sensitive to UV-C degradation than MAL. Residual  
511 concentrations remaining in the solution after 25 min irradiation were always greater for  
512 MAL than for ATR. ATR presents a maximum absorption between 220-230 nm, so with a  
513 sensitization effect more favorable than for MAL, which presents a maximum absorption  
514 wavelength at the limit of the UV-C region (Table 1) [8, 41].

515 In order to better understand the photodegradation process, the kinetic of degradation was  
516 evaluated for both ATR and MAL. The pseudo-first order kinetic modeling was applied in  
517 waste- and groundwater according to equation (6):

$$518 \quad \ln\left(\frac{C_t}{C_0}\right) = -k t \quad (6)$$

519 where  $C_0$  and  $C_t$  represent the concentration at time 0 and  $t$ , respectively, and  $k$  ( $\text{min}^{-1}$ ) is the  
520 pseudo-first order rate constant.

521 The values of the rate constants  $k$  and the coefficients of determination ( $r^2$ ) corresponding to  
522 the mathematical modeling (eq. 6) are summarized in Table 3. The pseudo-first order model  
523 fitted well with the experimental values for ATR and MAL and it was relevant for the  
524 different concentrations tested and whatever the water quality. Fig. 3 shows the plot obtained  
525 from equation (6) which is in accordance with the mean experimental values (obtained from  
526 duplicates).

527 Table 3: Pseudo-first order kinetic parameters for the photodegradation of MAL and ATR in  
 528 ground- and wastewater.

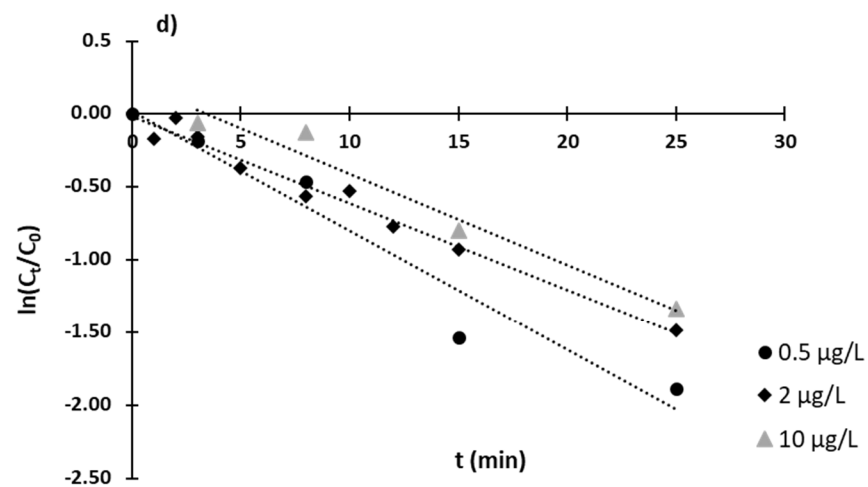
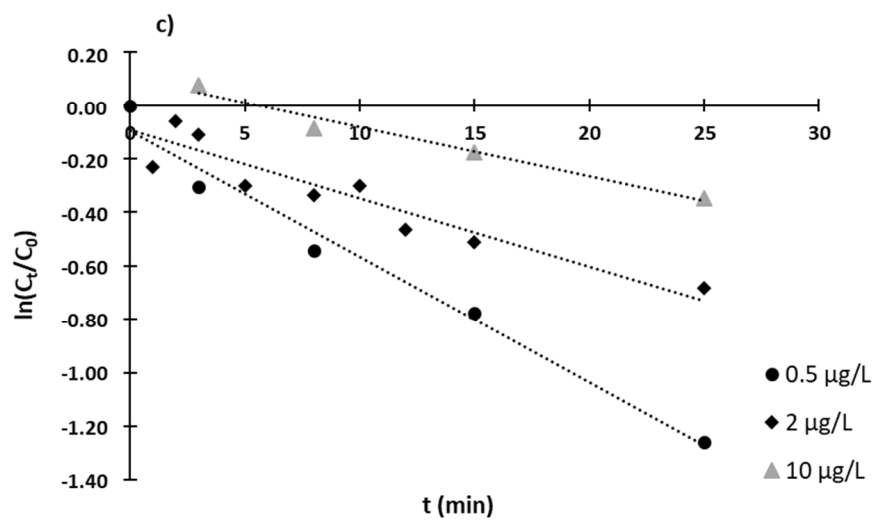
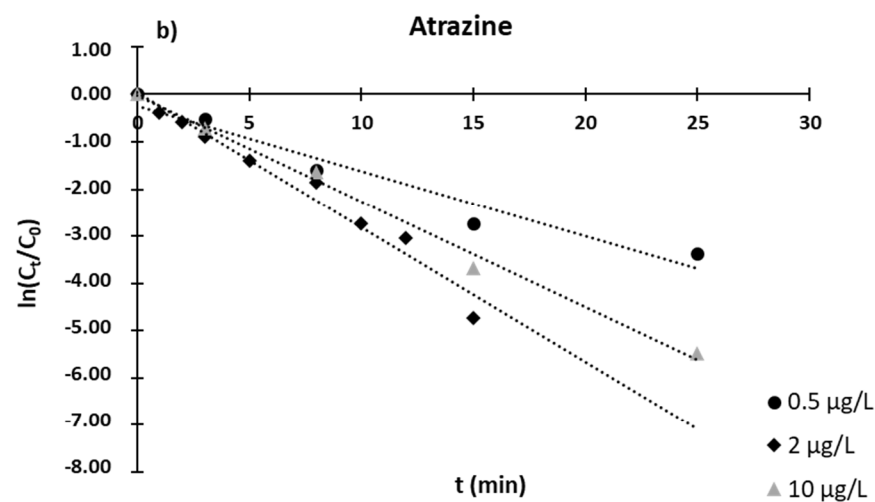
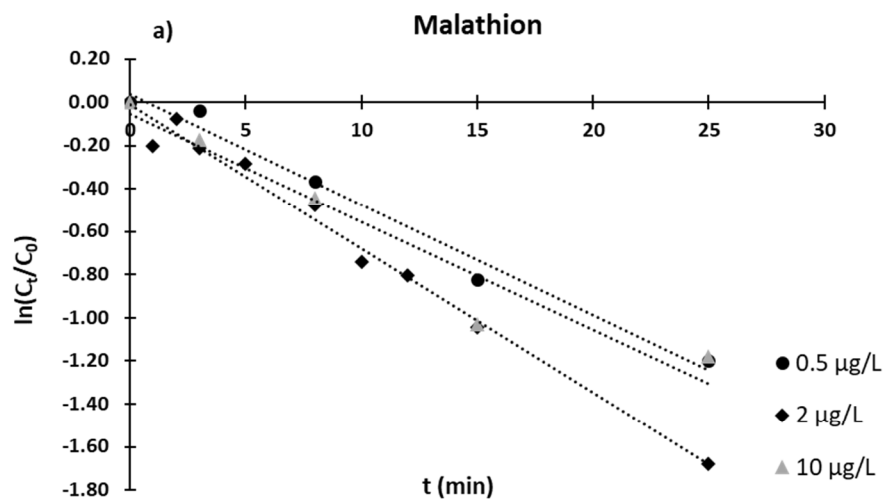
529

		Groundwater			Wastewater		
		k (min <sup>-1</sup> )	t <sub>1/2</sub> (min)	r <sup>2</sup>	k (min <sup>-1</sup> )	t <sub>1/2</sub> (min)	r <sup>2</sup>
Atrazine	0.5 µg L <sup>-1</sup>	0.1852	3.7	0.996	0.0817	8.5	0.945
	2 µg L <sup>-1</sup>	0.2847	2.4	0.970	0.0594	11.7	0.980
	10 µg L <sup>-1</sup>	0.2237	3.1	0.993	0.0622	11.9	0.964
Malathion	0.5 µg L <sup>-1</sup>	0.0512	13.5	0.980	0.0471	14.7	0.980
	2 µg L <sup>-1</sup>	0.0669	10.4	0.990	0.0257	27.0	0.870
	10 µg L <sup>-1</sup>	0.0456	15.2	0.992	0.0183	37.9	0.970

530

531

532 Figure 3: Plots of  $\ln(C_t/C_0)$  versus photoirradiation time for MAL and ATR in groundwater (a, b) and wastewater (c, d).



533  
534

535 Although the kinetics of the photochemical reactions can be complex because of the number  
536 of steps and the reactive species involved, the OH radical is usually regarded as the sole and  
537 rate limiting reactive species [46], which explains why the pseudo-first order kinetic could  
538 properly model the photodegradation kinetic. According to first-order kinetics, the time  
539 required for dissipating 50% of the initial concentration ( $t_{1/2}$ ) of MAL or ATR could be  
540 calculated by the equation (7):

$$541 \quad t_{1/2} = \frac{\ln 2}{k} \quad (7)$$

542 The values of  $t_{1/2}$  are given in Table 3. It shows that the first stage of ATR dissipation (for  
543 degrading at least one half of the molecules) was always faster than that of MAL.

544 In groundwater, the photodegradation process was less sensitive to the initial concentration of  
545 ATR or MAL than in wastewater, in the range 0.5-10  $\mu\text{g L}^{-1}$ . The constant rates  $k$  were only  
546 slightly higher at 2  $\mu\text{g L}^{-1}$  than at 0.5 or 10  $\mu\text{g L}^{-1}$  for both the molecules in groundwater. So  
547 the fluence corresponding to the dissipation of 50% of these pesticides in groundwater was  
548 between 887 and 1368 kJ per  $\text{m}^3$  of water for ATR and between 3845 and 5620 kJ per  $\text{m}^3$  for  
549 MAL, in the 0.5-10  $\mu\text{g L}^{-1}$  concentrations range. It is important to note here that continuous  
550 flow-through reactor studies for organic contaminants removal by UV-C photolysis are rare at  
551 the pilot scale, and that the results obtained for these pesticides are promising not only for the  
552 removal capacity but also for the energy expenditure [23]. For comparison, direct UV-C  
553 photolysis of a persistent pharmaceutical compound in drinking water showed degradation  
554 less than 6% at 15 min, in a bench-scale continuous flow-through reactor, corresponding to a  
555 fluence of 5000  $\text{kJ m}^{-3}$  [28].

556 For wastewater, the photodegradation of ATR and MAL was significantly slower than for  
557 groundwater. The time required to dissipate 50% of ATR was between 2.3 to 4.9 time longer  
558 in wastewater and between 2.6 to 6 times longer for MAL (Table 3). The exception was for  
559 MAL at 0.5  $\mu\text{g L}^{-1}$  whose  $t_{1/2}$  was quite the same for the two water qualities. So at the lowest

560 MAL concentration, the amount of ROS seemed to be sufficient to react with MAL even in  
561 the turbid water, but at MAL concentrations  $> 2 \mu\text{g L}^{-1}$ ,  $t_{1/2}$  increased drastically in wastewater  
562 which shows that generated active species were no longer sufficient (Table 3). The fluence  
563 corresponding to the dissipation of 50% ATR was between 3143 and 4400  $\text{kJ m}^{-3}$  of  
564 wastewater and increased from 5435 to 14014  $\text{kJ m}^{-3}$  of wastewater for MAL, depending on  
565 its initial concentration. Once again, the results obtained with the SurePure device are  
566 promising, even for a very turbid water. For comparison, the removal of ten pesticides (of  
567 which ATR) from leaching water containing DOM at pilot plant scale, using solar irradiation  
568 (UV-A to UV-C), was less than 20% after 60 min [39].

569

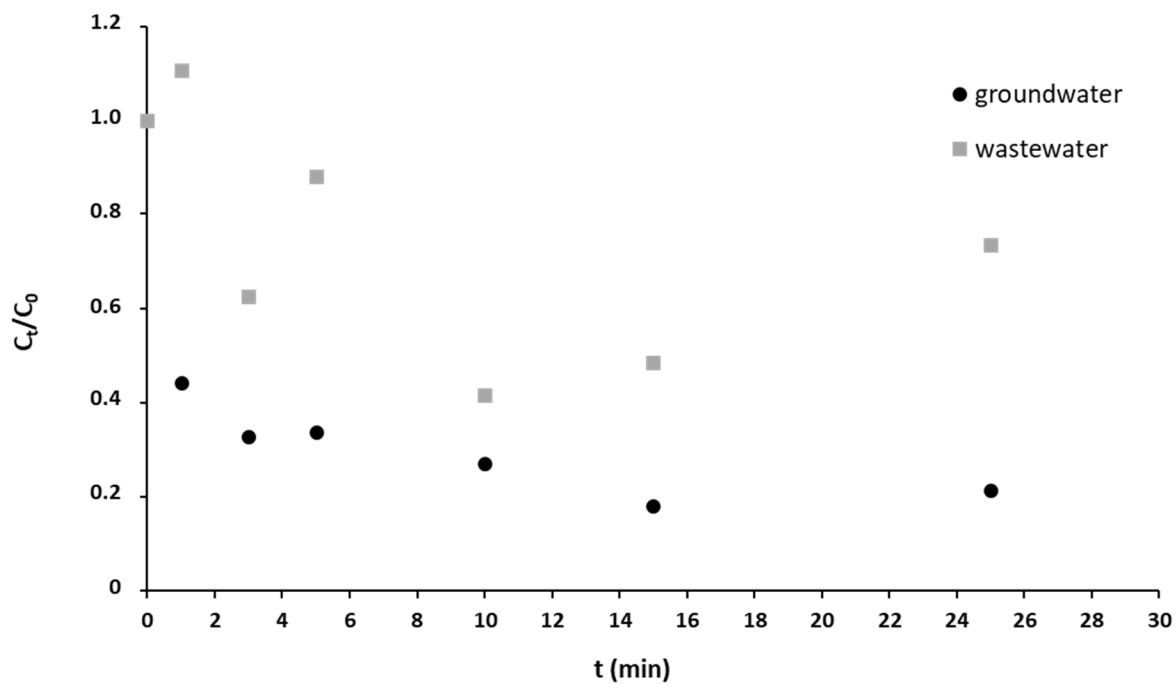
#### 570 *Dissipation of Glyphosate*

571 The photolytic dissipation of GLY was investigated for 30 minutes (Fig. 4). Some authors  
572 noted that no sign of direct photolysis was observed using UV-C irradiation for GLY at 50 mg  
573  $\text{L}^{-1}$  in pure water, which was justified by the absorption spectrum of GLY which is at the limit  
574 of the UV-C region [48]. However, the sample pH is important to take into account.  
575 McConnell *et al.* (1993) demonstrated that the absorption spectra of GLY could shift to  
576 higher values with a pH increase. Thus, the wavelength of the maximum absorption could  
577 shift to 214 nm for pHs higher than 7.0 [49]. In our case, treated waters were alkaline (7.9-  
578 8.2) which could explain a part of the GLY photosensitivity.

579

580 Figure 4: Dissipation of free GLY (initial spiking:  $10 \mu\text{g L}^{-1}$ ) in groundwater (n=3 tests) and  
581 wastewater (n=1 test) after UV-C irradiation (measured in the dissolved aqueous fraction  
582 from t=0).

583



584

585

586 As already mentioned (section 3.1), the direct photolysis of GLY in the very low  
587 concentration ranges, found in environmental water ( $\mu\text{g L}^{-1}$ ), is not well known, as  
588 photodegradation of GLY is more often studied using spiked GLY in the  $\text{mg L}^{-1}$  range and is  
589 usually assisted by photocatalysts in AOPs [50]. Here, the dissipation of GLY (spiked at 10  
590  $\mu\text{g L}^{-1}$ ) seemed very fast in groundwater because only one minute of treatment was enough to  
591 remove 57% of GLY (fluence =  $370 \text{ kJ m}^{-3}$ ) (Fig. 4). It is important to note that the reported  
592  $C_t/C_0$  values were calculated from the initial  $C_0$  concentration measured in the dissolved  
593 aqueous fraction at  $t_0$ , just before the irradiation began, so taking into account the GLY losses  
594 due to sorption (approximately 42% GLY was sorbed at  $t_0$  (section 3.1) and could not be  
595 measured in the dissolved fraction). The dissipation of free GLY was more than 75% after 10  
596 minutes of irradiation, corresponding to a fluence of  $3698 \text{ J m}^{-3}$  of treated groundwater (eq.  
597 (5)).

598 This fast and efficient dissipation of free GLY at low concentration ( $< 10 \mu\text{g L}^{-1}$ ) could not be  
599 fully explained by direct photolysis, but mainly by reactions with ROS such as hydroxyl or  
600 superoxide radicals, for instance, and also possibly by the presence of trace of metals and  
601 humic acids (HA) in groundwater. Groundwater may contain a small fraction of soluble  
602 organic colloids (DOM) composed of HA complexed to iron, manganese or aluminum,  
603 coming from soil lixiviation. The various aromatic compounds of HA, as polyphenols or  
604 organic acids, can form charge transfer complexes with some herbicides, further sensitising  
605 them for the photodegradation [51]. Also, it is known that inorganic Fe or Mn elements can  
606 act as catalysts for GLY degradation by oxidation in photodegradation or electro-Fenton like  
607 processes [52, 53]. In particular, HA and  $\text{Fe}^{3+}$  complexes can sensitize aquatic  
608 photodegradation of GLY, with HA interacting with  $\text{Fe}^{3+}$  to produce more hydroxyl radicals,  
609 causing the C-N and C-P bonds cleavage to form phosphate [53]. It should be noted here that  
610 AMPA apparition could not be measured during the exposure of GLY to UV-C.



611 It must be underlined that the results obtained for GLY removal with the SurePure device are  
612 very encouraging. According to the review from Diez *et al.* (2019), there was just few  
613 publications on agrochemicals degradation by UV-C light at the pilot scale without catalyst  
614 [23]. The cited authors reached a degradation of 30% in 100 minutes for a pesticide and 5% in  
615 100 minutes for a fungicide for 19 L of treated water, demonstrating that 75% GLY removal  
616 after 10 min irradiation, obtained in this work, is promising. Moreover, it is important to note  
617 that these cited works were investigated in pure water and not in groundwater (or wastewater)  
618 like in this study. At last, experiments on GLY using UV-C irradiation at the pilot scale are  
619 even more rare and Jönsson *et al.* mentioned that the removal of GLY, spiked in drinking  
620 water at  $3 \mu\text{g L}^{-1}$ , was not exceeding 36% after 7 days of treatment with UV-C irradiation in a  
621 flow through system [54].

622 For wastewater, the performance of photolysis was also interesting with more than 50% of the  
623 initial concentration of free GLY removed from the water after 10 minutes exposure and a  
624 fluence of  $3698 \text{ kJ m}^{-3}$  (Fig. 4). However, after 10 minutes, the concentration of soluble GLY  
625 increased in the pilot, indicating that a part of GLY was again released in the aqueous phase.  
626 Compared with groundwater, an important part of GLY was sorbed to the pilot surfaces  
627 (stainless steel and quartz tubes) as well as to the high amount of SPM. Approximately 80%  
628 GLY was sorbed to all the solid surfaces (known initial spiked amounts were compared with  
629 those measured after equilibrium of wastewater into the pilot and the water collected at  $t_0$ , just  
630 before the irradiation began). It has been reported that GLY and AMPA were more frequently  
631 found associated with SPM than in the soluble phase despite their high solubility, with  
632 partition coefficients in the range of  $81\text{-}7564 \text{ L kg}^{-1}$  which is significantly higher than those of  
633 ATR and MAL (Table 1) [9, 31, 55]. Therefore, in the case of the turbid wastewater, a  
634 photodegradation of the soluble GLY fraction may occur rapidly, although SPM limit the  
635 interaction with photons and the generation of hydroxyl radicals with the aid of HA from

636 DOM. However, particulate matter tended to release sorbed GLY, possibly at each water  
637 cycle and because the solid/liquid partition was continuously modified in this dynamic  
638 system. Unfortunately, GLY disappearance was lower than GLY release. It means that UV-C  
639 irradiation must be significantly longer than 30 min to eliminate all the dissolved GLY  
640 molecules from the turbid water.

641

## 642 **Conclusions**

643 This study investigated the degradation of ATR, MAL and GLY pesticides by direct UV-C  
644 photolysis in order to develop a circular economic model to clean water used in agriculture.  
645 The direct photolysis, applied in a continuous flow-through system which could treat 40 L  
646 water, was investigated on natural spiked ground- and wastewater. For diluted ( $0.5 \mu\text{g L}^{-1}$ )  
647 and more concentrated ( $10 \mu\text{g L}^{-1}$ ) solutions, ATR was completely eliminated after 15  
648 minutes from groundwater while 80% was removed from the more turbid wastewater after 25  
649 minutes treatment. The GC-MS analysis demonstrated that ATR was not quantitatively  
650 converted to DIA or DIE and that trace levels of these transformation products were not  
651 eliminated by UV-C treatment in both water samples. For MAL, 70 to 80% (as a function of  
652 the initial concentration) was removed in 25 minutes from the groundwater by photolytic  
653 oxidation. For wastewater, the initial concentration of MAL was important on the  
654 performance of the photolytic process. The dissipation of GLY at concentrations ( $10 \mu\text{g L}^{-1}$ )  
655 higher than those found in natural groundwater was promising because it was quantitatively  
656 eliminated after 10 minutes of irradiation (>75%), possibly with the aid of HA. In wastewater  
657 containing high amount of SPM, the UV-C treatment was less efficient because GLY was  
658 mainly adsorbed to particles which obstruct the photodegradation process. It seems that only  
659 dissolved GLY could be photodegraded at low concentration and the continuous release of  
660 GLY from particles in the dynamic UV-DS system was an obstacle to its rapid quantitative  
661 elimination. This study therefore, demonstrated that the UV-C treatment applied to large

662 volumes of water, using a turbulent flow and the multiple-lamp system, was effective to  
663 rapidly and quantitatively remove some herbicides and pesticides by direct photolytic  
664 oxidation, without added catalysts, when the turbidity of the treated water is limited.

665 As transformation products can sometimes be more toxic than parent pesticides, the ability of  
666 the UV-C treatment to remove quantitatively problematic pesticides in water will need, in the  
667 future, to be supported by toxicity assays and researches on potential ecological effects.

668

669

## 670 **Acknowledgements**

671 The authors acknowledge the Labex SYNORG (ANR-11-LABX-0029), the Région  
672 Normandie (CRUNCH and Sésa network) and ERDF (Cos-Sésa) for support.

673

## 674 **References**

- 675 [1] E. Villanneau, N.P.A. Saby, D. Arrouays, C.C. Jolivet, L. Boulonne, G. Caria, E. Barriuso, A. Bispo, O.  
676 Briand, Spatial distribution of lindane in topsoil of Northern France, *Chemosphere*, 77 (2009) 1249-  
677 1255. <https://doi.org/10.1016/j.chemosphere.2009.08.060>
- 678 [2] V.C. Schreiner, E. Szöcs, A.K. Bhowmik, M.G. Vijver, R.B. Schäfer, Pesticide mixtures in streams of  
679 several European countries and the USA, *Science of The Total Environment*, 573 (2016) 680-689.  
680 <https://doi.org/10.1016/j.scitotenv.2016.08.163>
- 681 [3] F.J. Benitez, F.J. Real, J.L. Acero, C. Garcia, Photochemical oxidation processes for the elimination  
682 of phenyl-urea herbicides in waters, *Journal of hazardous materials*, 138 (2006) 278-287.  
683 <https://doi.org/10.1016/j.jhazmat.2006.05.077>
- 684 [4] M.P. Silva, A.P. dos Santos Batista, S.I. Borrely, V.H.O. Silva, A.C.S.C. Teixeira, Photolysis of atrazine  
685 in aqueous solution: role of process variables and reactive oxygen species, *Environmental Science  
686 and Pollution Research*, 21 (2014) 12135-12142. <https://doi.org/10.1007/s11356-014-2881-0>
- 687 [5] N. Chen, D. Valdes, C. Marlin, P. Ribstein, F. Alliot, E. Aubry, H. Blanchoud, Transfer and  
688 degradation of the common pesticide atrazine through the unsaturated zone of the Chalk aquifer  
689 (Northern France), *Environmental Pollution*, 255 (2019) 113125.  
690 <https://doi.org/10.1016/j.envpol.2019.113125>
- 691 [6] L. Carles, H. Gardon, L. Joseph, J. Sanchís, M. Farré, J. Artigas, Meta-analysis of glyphosate  
692 contamination in surface waters and dissipation by biofilms, *Environment International*, 124 (2019)  
693 284-293. <https://doi.org/10.1016/j.envint.2018.12.064>
- 694 [7] J. Dollinger, C. Dagès, M. Voltz, Glyphosate sorption to soils and sediments predicted by  
695 pedotransfer functions, *Environmental Chemistry Letters*, 13 (2015) 293-307.  
696 <https://doi.org/10.1007/s10311-015-0515-5>
- 697 [8] L. Velkoska-Markovska, B. Petanovska-Ilievska, A. Markovski, Application of High Performance  
698 Liquid Chromatography to the Analysis of Pesticide Residues in Apple Juice, *Contemporary  
699 Agriculture*, 67 (2018) 93-102. doi:10.2478/contagri-2018-0014

700 [9] R.L. Glass, Adsorption of glyphosate by soils and clay minerals, *Journal of Agricultural and Food*  
701 *Chemistry*, 35 (1987) 497-500. <https://doi.org/10.1021/jf00076a013>

702 [10] G.-M. Momplaisir, C.G. Rosal, E.M. Heithmar, K.E. Varner, L.A. Riddick, D.F. Bradford, N.G.  
703 Tallent-Halsell, Development of a solid phase extraction method for agricultural pesticides in large-  
704 volume water samples, *Talanta*, 81 (2010) 1380-1386. <https://doi.org/10.1016/j.talanta.2010.02.038>

705 [11] S. Barrek, C. Cren-Olivé, L. Wiest, R. Baudot, C. Arnaudguilhem, M.-F. Grenier-Loustalot, Multi-  
706 residue analysis and ultra-trace quantification of 36 priority substances from the European Water  
707 Framework Directive by GC-MS and LC-FLD-MS/MS in surface waters, *Talanta*, 79 (2009) 712-722.  
708 <https://doi.org/10.1016/j.talanta.2009.04.058>

709 [12] R. Carabias-Martínez, E. Rodríguez-Gonzalo, E. Herrero-Hernández, F.J. Sánchez-San Román,  
710 M.G. Prado Flores, Determination of herbicides and metabolites by solid-phase extraction and liquid  
711 chromatography: Evaluation of pollution due to herbicides in surface and groundwaters, *Journal of*  
712 *Chromatography A*, 950 (2002) 157-166. [https://doi.org/10.1016/S0021-9673\(01\)01613-2](https://doi.org/10.1016/S0021-9673(01)01613-2)

713 [13] C. Hao, D. Morse, F. Morra, X. Zhao, P. Yang, B. Nunn, Direct aqueous determination of  
714 glyphosate and related compounds by liquid chromatography/tandem mass spectrometry using  
715 reversed-phase and weak anion-exchange mixed-mode column, *Journal of Chromatography A*, 1218  
716 (2011) 5638-5643. <https://doi.org/10.1016/j.chroma.2011.06.070>

717 [14] B. Le Bot, K. Colliaux, D. Pelle, C. Briens, R. Seux, M. Clément, Optimization and performance  
718 evaluation of the analysis of glyphosate and AMPA in water by HPLC with fluorescence detection,  
719 *Chromatographia*, 56 (2002) 161-164. <https://doi.org/10.1007/BF02493205>

720 [15] T. Arkan, A. Csámpai, I. Molnár-Perl, Alkylsilyl derivatization of glyphosate and  
721 aminomethylphosphonic acid followed by gas chromatography mass spectrometry, *Microchemical*  
722 *Journal*, 125 (2016) 219-223. <https://doi.org/10.1016/j.microc.2015.11.027>

723 [16] J. Jiang, C.A. Lucy, Determination of glyphosate using off-line ion exchange preconcentration and  
724 capillary electrophoresis-laser induced fluorescence detection, *Talanta*, 72 (2007) 113-118.  
725 <https://doi.org/10.1016/j.talanta.2006.10.001>

726 [17] C.E. Ramirez, S. Bellmund, P.R. Gardinali, A simple method for routine monitoring of glyphosate  
727 and its main metabolite in surface waters using lyophilization and LC-FLD+MS/MS. Case study: canals  
728 with influence on Biscayne National Park, *Science of The Total Environment*, 496 (2014) 389-401.  
729 <https://doi.org/10.1016/j.scitotenv.2014.06.118>

730 [18] C. Hidalgo, C. Rios, M. Hidalgo, V. Salvadó, J.V. Sancho, F. Hernández, Improved coupled-column  
731 liquid chromatographic method for the determination of glyphosate and aminomethylphosphonic  
732 acid residues in environmental waters, *Journal of Chromatography A*, 1035 (2004) 153-157.  
733 <https://doi.org/10.1016/j.chroma.2004.02.044>

734 [19] J. Patsias, A. Papadopoulou, E. Papadopoulou-Mourkidou, Automated trace level determination  
735 of glyphosate and aminomethyl phosphonic acid in water by on-line anion-exchange solid-phase  
736 extraction followed by cation-exchange liquid chromatography and post-column derivatization,  
737 *Journal of Chromatography A*, 932 (2001) 83-90. [https://doi.org/10.1016/S0021-9673\(01\)01253-5](https://doi.org/10.1016/S0021-9673(01)01253-5)

738 [20] A. Tufail, W.E. Price, M. Mohseni, B.K. Pramanik, F.I. Hai, A critical review of advanced oxidation  
739 processes for emerging trace organic contaminant degradation: Mechanisms, factors, degradation  
740 products, and effluent toxicity, *Journal of Water Process Engineering*, (2020) 101778.  
741 <https://doi.org/10.1016/j.jwpe.2020.101778>

742 [21] J.-L. Shie, C.-H. Lee, C.-S. Chiou, C.-T. Chang, C.-C. Chang, C.-Y. Chang, Photodegradation kinetics  
743 of formaldehyde using light sources of UVA, UVC and UVLED in the presence of composed silver  
744 titanium oxide photocatalyst, *Journal of Hazardous Materials*, 155 (2008) 164-172.  
745 <https://doi.org/10.1016/j.jhazmat.2007.11.043>

746 [22] C. Bertoldi, A.G. Rodrigues, A.N. Fernandes, Removal of endocrine disrupters in water under  
747 artificial light: the effect of organic matter, *Journal of Water Process Engineering*, 27 (2019) 126-133.  
748 <https://doi.org/10.1016/j.jwpe.2018.11.016>

749 [23] A.M. Díez, M.A. Sanromán, M. Pazos, New approaches on the agrochemicals degradation by UV  
750 oxidation processes, *Chemical Engineering Journal*, 376 (2019) 120026.  
751 <https://doi.org/10.1016/j.cej.2018.09.187>

752 [24] R.O. Ramos, M.V.C. Albuquerque, W.S. Lopes, J.T. Sousa, V.D. Leite, Degradation of indigo  
753 carmine by photo-Fenton, Fenton, H<sub>2</sub>O<sub>2</sub>/UV-C and direct UV-C: Comparison of pathways, products  
754 and kinetics, *Journal of Water Process Engineering*, 37 (2020) 101535.  
755 <https://doi.org/10.1016/j.jwpe.2020.101535>

756 [25] E. Blázquez, C. Rodríguez, J. Ródenas, N. Navarro, C. Riquelme, R. Rosell, J. Campbell, J.  
757 Crenshaw, J. Segalés, J. Pujols, J. Polo, Evaluation of the effectiveness of the SurePure Turbulator  
758 ultraviolet-C irradiation equipment on inactivation of different enveloped and non-enveloped viruses  
759 inoculated in commercially collected liquid animal plasma, *PLOS ONE*, 14 (2019) e0212332.  
760 [10.1371/journal.pone.0212332](https://doi.org/10.1371/journal.pone.0212332)

761 [26] N. Bustos, A. Cruz-Alcalde, A. Iriel, A. Fernández Cirelli, C. Sans, Sunlight and UVC-254 irradiation  
762 induced photodegradation of organophosphorus pesticide dichlorvos in aqueous matrices, *Sci Total  
763 Environ*, 649 (2019) 592-600. <https://doi.org/10.1016/j.scitotenv.2018.08.254>

764 [27] M. Bavcon Kralj, U. Černigoj, M. Franko, P. Trebše, Comparison of photocatalysis and photolysis  
765 of malathion, isomalathion, malaaxon, and commercial malathion—Products and toxicity studies,  
766 *Water Research*, 41 (2007) 4504-4514. <https://doi.org/10.1016/j.watres.2007.06.016>

767 [28] P. Somathilake, J.A. Dominic, G. Achari, C.H. Langford, J.-H. Tay, Use of low pressure mercury  
768 lamps with H<sub>2</sub>O<sub>2</sub> and TiO<sub>2</sub> for treating carbamazepine in drinking water: Batch and continuous flow  
769 through experiments, *Journal of Water Process Engineering*, 26 (2018) 230-236.  
770 <https://doi.org/10.1016/j.jwpe.2018.10.015>

771 [29] R. Ahmad, Z. Ahmad, A.U. Khan, N.R. Mastoi, M. Aslam, J. Kim, Photocatalytic systems as an  
772 advanced environmental remediation: Recent developments, limitations and new avenues for  
773 applications, *Journal of Environmental Chemical Engineering*, 4 (2016) 4143-4164.  
774 <https://doi.org/10.1016/j.jece.2016.09.009>

775 [30] F. Alberini, M.J.H. Simmons, D.J. Parker, T. Koutchma, Validation of hydrodynamic and microbial  
776 inactivation models for UV-C treatment of milk in a swirl-tube 'SurePure Turbulator™', *Journal of  
777 Food Engineering*, 162 (2015) 63-69. <https://doi.org/10.1016/j.jfoodeng.2015.04.009>

778 [31] T.M. Mac Loughlin, M.L. Peluso, V.C. Aparicio, D.J.G. Marino, Contribution of soluble and  
779 particulate-matter fractions to the total glyphosate and AMPA load in water bodies associated with  
780 horticulture, *Science of The Total Environment*, 703 (2020) 134717.  
781 <https://doi.org/10.1016/j.scitotenv.2019.134717>

782 [32] I. Hanke, H. Singer, J. Hollender, Ultratrace-level determination of glyphosate,  
783 aminomethylphosphonic acid and glufosinate in natural waters by solid-phase extraction followed by  
784 liquid chromatography–tandem mass spectrometry: performance tuning of derivatization,  
785 enrichment and detection, *Analytical and Bioanalytical Chemistry*, 391 (2008) 2265-2276.  
786 <https://doi.org/10.1007/s00216-008-2134-5>

787 [33] S. Wang, B. Liu, D. Yuan, J. Ma, A simple method for the determination of glyphosate and  
788 aminomethylphosphonic acid in seawater matrix with high performance liquid chromatography and  
789 fluorescence detection, *Talanta*, 161 (2016) 700-706. <https://doi.org/10.1016/j.talanta.2016.09.023>

790 [34] T.V. Nedelkoska, G.K.C. Low, High-performance liquid chromatographic determination of  
791 glyphosate in water and plant material after pre-column derivatisation with 9-fluorenylmethyl  
792 chloroformate, *Analytica Chimica Acta*, 511 (2004) 145-153.  
793 <https://doi.org/10.1016/j.aca.2004.01.027>

794 [35] R.J. Vreeken, P. Speksnijder, I. Bobeldijk-Pastorova, T.H.M. Noij, Selective analysis of the  
795 herbicides glyphosate and aminomethylphosphonic acid in water by on-line solid-phase extraction–  
796 high-performance liquid chromatography–electrospray ionization mass spectrometry, *Journal of  
797 Chromatography A*, 794 (1998) 187-199. [https://doi.org/10.1016/S0021-9673\(97\)01129-1](https://doi.org/10.1016/S0021-9673(97)01129-1)

798 [36] W.C. Koskinen, L.J. Marek, K.E. Hall, Analysis of glyphosate and aminomethylphosphonic acid in  
799 water, plant materials and soil, *Pest Management Science*, 72 (2016) 423-432.  
800 <https://doi.org/10.1002/ps.4172>

801 [37] Y.S. Hu, Y.Q. Zhao, B. Sorohan, Removal of glyphosate from aqueous environment by adsorption  
802 using water industrial residual, *Desalination*, 271 (2011) 150-156.  
803 <https://doi.org/10.1016/j.desal.2010.12.014>

804 [38] I. Freuze, A. Jadas-Hecart, A. Royer, P.-Y. Communal, Influence of complexation phenomena with  
805 multivalent cations on the analysis of glyphosate and aminomethyl phosphonic acid in water, *Journal*  
806 *of Chromatography A*, 1175 (2007) 197-206. <https://doi.org/10.1016/j.chroma.2007.10.092>  
807 [39] M.P. Silva, A.P. dos Santos Batista, S.I. Borrelly, V.H.O. Silva, A.C.S.C. Teixeira, Photolysis of  
808 atrazine in aqueous solution: role of process variables and reactive oxygen species.  
809 [40] G.V. Buxton, C.L. Greenstock, W.P. Helman, A.B. Ross, Critical Review of rate constants for  
810 reactions of hydrated electrons, hydrogen atoms and hydroxyl radicals ( $\cdot\text{OH}/\cdot\text{O}^-$  in Aqueous Solution,  
811 *Journal of Physical and Chemical Reference Data*, 17 (1988) 513-886. 10.1063/1.555805  
812 [41] H. Prosen, L. Zupančič-Kralj, Evaluation of photolysis and hydrolysis of atrazine and its first  
813 degradation products in the presence of humic acids, *Environmental Pollution*, 133 (2005) 517-529.  
814 <https://doi.org/10.1016/j.envpol.2004.06.015>  
815 [42] A.J. Moreira, A.C. Borges, L.F.C. Gouvea, T.C.O. MacLeod, G.P.G. Freschi, The process of atrazine  
816 degradation, its mechanism, and the formation of metabolites using UV and UV/MW photolysis,  
817 *Journal of Photochemistry and Photobiology A: Chemistry*, 347 (2017) 160-167.  
818 <https://doi.org/10.1016/j.jphotochem.2017.07.022>  
819 [43] D.W. Kolpin, E.M. Thurman, S.M. Linhart, Finding minimal herbicide concentrations in ground  
820 water? Try looking for their degradates, *Science of The Total Environment*, 248 (2000) 115-122.  
821 [https://doi.org/10.1016/S0048-9697\(99\)00535-5](https://doi.org/10.1016/S0048-9697(99)00535-5)  
822 [44] J.A. Khan, X. He, N.S. Shah, M. Sayed, H.M. Khan, D.D. Dionysiou, Degradation kinetics and  
823 mechanism of desethyl-atrazine and desisopropyl-atrazine in water with OH and  $\text{SO}_4^-$  based-AOPs,  
824 *Chemical Engineering Journal*, 325 (2017) 485-494. <https://doi.org/10.1016/j.cej.2017.05.011>  
825 [45] W. Li, Y. Zhao, X. Yan, J. Duan, C.P. Saint, S. Beecham, Transformation pathway and toxicity  
826 assessment of malathion in aqueous solution during UV photolysis and photocatalysis, *Chemosphere*,  
827 234 (2019) 204-214. <https://doi.org/10.1016/j.chemosphere.2019.06.058>  
828 [46] S. Navarro, J. Fenoll, N. Vela, E. Ruiz, G. Navarro, Removal of ten pesticides from leaching water  
829 at pilot plant scale by photo-Fenton treatment, *Chemical Engineering Journal*, 167 (2011) 42-49.  
830 <https://doi.org/10.1016/j.cej.2010.11.105>  
831 [47] L. Varanasi, E. Coscarelli, M. Khaksari, L.R. Mazzoleni, D. Minakata.  
832 [48] A. Manassero, C. Passalia, A.C. Negro, A.E. Cassano, C.S. Zalazar, Glyphosate degradation in  
833 water employing the  $\text{H}_2\text{O}_2/\text{UVC}$  process, *Water Research*, 44 (2010) 3875-3882.  
834 <https://doi.org/10.1016/j.watres.2010.05.004>  
835 [49] J.S. McConnell, R.M. McConnell, Ultraviolet Spectra of Acetic Acid, Glycine, and Glyphosate,  
836 *Journal of the Arkansas Academy of Science*, 47 (1993) 73-76.  
837 [50] D. Feng, A. Soric, O. Boutin, Treatment technologies and degradation pathways of glyphosate: A  
838 critical review, *Science of The Total Environment*, 742 (2020) 140559.  
839 <https://doi.org/10.1016/j.scitotenv.2020.140559>  
840 [51] K. Lányi, P. Laczay, J. Lehel, Effects of some naturally occurring substances on the  
841 photodegradation of herbicide methabenzthiazuron, *Journal of Environmental Chemical Engineering*,  
842 4 (2016) 123-129. <https://doi.org/10.1016/j.jece.2015.11.002>  
843 [52] B. Balci, M.A. Oturan, N. Oturan, I. Sirés, Decontamination of Aqueous Glyphosate,  
844 (Aminomethyl)phosphonic Acid, and Glufosinate Solutions by Electro-Fenton-like Process with  $\text{Mn}^{2+}$   
845 as the Catalyst, *Journal of Agricultural and Food Chemistry*, 57 (2009) 4888-4894.  
846 <https://doi.org/10.1021/jf900876x>  
847 [53] J. Liu, J. Fan, T. He, X. Xu, Y. Ai, H. Tang, H. Gu, T. Lu, Y. Liu, G. Liu, The mechanism of aquatic  
848 photodegradation of organophosphorus sensitized by humic acid- $\text{Fe}^{3+}$  complexes, *Journal of*  
849 *Hazardous Materials*, 384 (2020) 121466. <https://doi.org/10.1016/j.jhazmat.2019.121466>  
850 [54] J. Jönsson, R. Camm, T. Hall, Removal and degradation of glyphosate in water treatment: a  
851 review, *Journal of Water Supply: Research and Technology-Aqua*, 62 (2013) 395-408.  
852 10.2166/aqua.2013.080  
853 [55] R. Kanissery, B. Gairhe, D. Kadyampakeni, O. Batuman, F. Alferéz, Glyphosate: Its Environmental  
854 Persistence and Impact on Crop Health and Nutrition, *Plants*, 8 (2019).  
855 <https://doi.org/10.3390/plants8110499>

